Magnesium Technology 2012
Edited by: Suveen N. Mathaudhu, Wim H. Sillekens, Neale R. Neelameggham, and Norbert Hort
TMS (The Minerals, Metals & Materials Society), 2012

EFFECTS OF DIRECT EXTRUSION PROCESS ON MICROSTRUCTURE, TEXTURE EVOLUTION AND YIELD STRENGTH OF MAGNESIUM ALLOY AZ31

Shiyao Huang[1], Mei Li[1], John E. Allison[2], Shaorui Zhang[3], Dayong Li[3], Yinghong Peng[3]

[1]Research and Advanced Engineering Laboratory, Ford Motor Company, Dearborn, MI 48121, USA
[2]Department of Material Science and Engineering, University of Michigan, Ann Arbor, MI 48109, USA
[3]School of Mechanical Engineering, Shanghai Jiao Tong University, Shanghai 200240, P.R. China

Keywords: Magnesium alloy AZ31, Extrusion, Microstructure, Texture, Yield strength

Abstract

Direct extrusions of commercial casting AZ31 alloy were carried out at elevated temperatures with different extrusion velocities. Microstructure and texture distribution of extruded rods were investigated with optical microscopy (OM) and electron backscattered diffraction (EBSD). Tensile tests were conducted at room temperature using samples from both casting billets and extruded rods. The experimental yield strength can not be solely described by average grain size. In this paper, the grain size and orientation in the extruded samples were characterized by EBSD, and Hall-Petch equation was applied to each individual grain with the input from EBSD results (individual grain size and orientation). The yield strength of tensile sample (polycrystalline aggregate) and individual grain was related by Taylor assumption. The predicted yield strength showed the same trend as experiment results.

Introduction

The development of magnesium alloys for the automotive and aerospace industry has attracted significant attention due to its light weight and consequent potential to reduce both fuel consumption and green house effect, in addition to their excellent damping capacity and recyclability. Major commercial magnesium alloys are produced either as cast products (e.g. die, sand and mold castings) or wrought products (e.g. extrusion, stamping, forging and rolling). Wrought Mg alloys are of special interest for some applications due to the improved properties compared with casting products, such as fracture toughness, yield strength, fatigue strength, ductility, and corrosion behavior [1-5]. Although extrusion process of Mg alloy AZ31 has been studied extensively, most researches are concentrated on equal channel angular extrusion (ECAE) [6,7], hydrostatic extrusion [8,9], cyclic extrusion [10], and indirect extrusion [11,12]. Detailed studies on microstructure development and texture evolution during direct extrusion process of AZ31 alloy are still rare.

The effects of grain size and texture distribution of magnesium alloy on yield strength have been studied widely [13-17]. The relationship between yield strength σ and grain size d could be empirically described by the Hall-Petch equation (1) [18,19],

$$\sigma = \sigma_0 + kd^{-1/2} \quad (1)$$

where σ_0 represents the friction stress for dislocation movement, and k is the constant representing the grain boundary as an obstacle for dislocations to slip across the grain boundaries [17]. By plotting yield strength σ against average grain size d, σ_0 and k can be determined by parameter fitting. However, this fitting method does not take into account of texture explicitly, and thus the effect of texture on yield strength is not clearly considered. Furthermore, the deformation of casting AZ31 alloy results in very inhomogeneous grain size distribution and textured grain orientation, which makes it necessary to consider the contribution of the grain size and its orientation of each grain to yield strength. Fromm [20] introduced grain size and orientation distribution function (GSODF) into crystal plasticity model to predict large yield strength anisotropy of rolled α-titanium. But this method requires experimental data from multi-section orientation imaging microscopy and the calculation of GSODF is complex.

In the present study, effects of hot extrusion process on microstructure, texture distribution and yield strength of AZ31 alloy were studied. Forward extrusions of AZ31 were carried out at 9 deformation conditions. Microstructure and texture distribution of extruded rods were investigated with optical microscopy (OM) and electron backscattered diffraction (EBSD). Then tensile tests were conducted at room temperature using samples from both casting billets and extruded rods. Hall-Petch equation was applied to each individual grain with the input of EBSD results (individual grain size and orientation), the yield strength of tensile sample (polycrystalline aggregate) and individual grain was related by Taylor assumption.

Experimental Procedures

Commercial direct chill (DC) casting feedstock of AZ31 alloy was machined into billets (Φ100mm) for extrusion trials. The alloy compositions are listed in Table I. Direct extrusion tests were carried out at 9 deformation conditions with combination of different temperatures (643K, 673K and 703K) and extrusion speeds (0.8 m/min, 1.4 m/min and 2.2 m/min). The extruded rods (Φ40mm) were cooled down in air after extrusion.

Specimens for optical microscopy (OM) were mounted in epoxy resin, grounded with 1200 grit SiC paper, mechanically polished using 6, 3 and 1 μm diamond paste and 0.3, 0.05 μm alumina solution. Specimens were etched for 5s in acetic picral (10ml acetic, 10ml Distilled Water, 70 ml picral).

Table I The Compositions of AZ31 (wt%)

Alloy	Mg	Al	Be	Cu	Fe	Mn	Pb	Si	Zn
AZ31	Bal.	2.66	<0.0005	<0.005	0.01	0.36	<0.01	0.01	0.84

Specimens for electron backscattered diffraction (EBSD) were ground with 2000 grit SiC paper, followed by mechanically polishing with 3μm diamond paste. Specimens were prepared by electro-polishing in AC2 electrolyte for the final stage. The microstructure was imaged using a LEO 1450-VP SEM. Grain orientations were examined and analyzed using Zeiss Suppa 55VP SEM equipped with HKL Channel 5 system.

In order to measure the mechanical properties improvement after extrusion process, tensile tests were performed on an Instron tensile testing machine at room temperature. Three samples were tested for each extrusion condition. Dimensions of tensile test sample were shown in Figure 1.

All specimens for OM, EBSD and tensile testing were cut from center of the extruded rods, parallel to the extrusion direction.

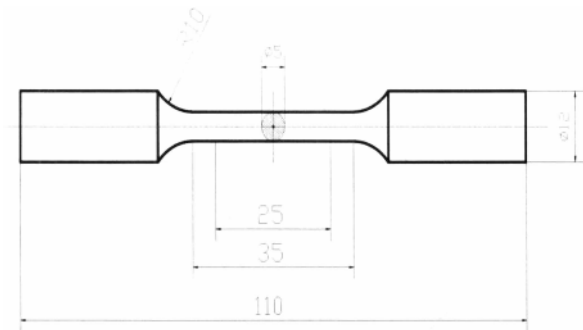

Figure 1. Dimensions of tensile test sample (in millimeters)

Results and Discussion

Microstructure Development

Figure 2 shows the microstructure of AZ31 casting billets used in this study. It consists of large grain with mean grain size of about 200μm. Figure 3 shows the microstructures of the AZ31 rods extruded at different conditions. The extruded microstructures are very inhomogeneous with averaged grain size decreasing dramatically compared to casting billet. Large grains in cast billets have been elongated along extrusion direction. Large amount of small grains formed at the junctions of grain boundaries. Fine DRX grains also forms "necklace" structure along grain boundaries.

Figure 2. Microstructure of casting AZ31 billet

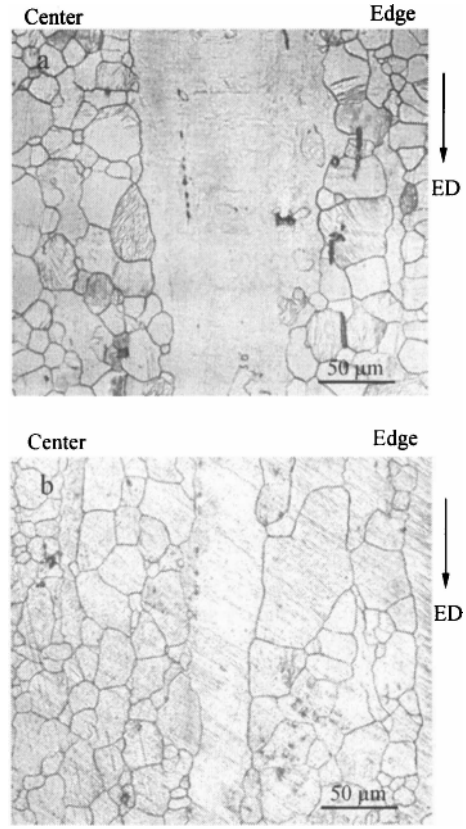

Figure 3. Microstructure of extruded rods. (a) Temperature=643K, velocity=1.4m/min. (b) Temperature=673K, velocity=1.4m/min.

Grain boundaries act as obstacles to the movement of dislocations. Thus, dislocations accumulate and subsequently generate local stress concentrations on the grain boundaries, resulting in the generation of serrated boundaries. The development of serrated grain boundaries leads to the nucleation of DRX by bulging [21]. The serrated grain boundaries are frequently observed in extruded rods, as shown in Figure 3. Figure 4 illustrates two examples of nucleation by bulging. In Figure 4(a) and Figure 4(b), the bulging area of grain A is almost cut off by grain B and grain C, the potential nucleation area is indicated by A^*.

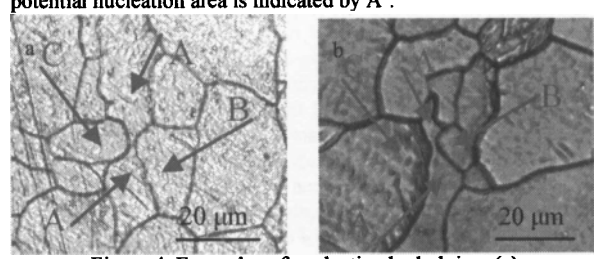

Figure 4. Examples of nucleation by bulging. (a) Temperature=673K, velocity=1.4m/min. (b) Temperature=673K, velocity=2.2m/ min.

During compression test of the as-cast AZ31 alloy, Beer [22] reported a process where a progressive increase in misorientation from the center to the boundary of grain and the conversion of low angle boundaries into the high angle ones. In the current study of

direct extrusion process, the development of high angle grain boundary is also observed. As indicated by white arrow in Figure 5, the serrated grain boundaries in the elongated grain can gradually increase in misorientation, inducing the sub-boundaries behind bulges. Further rotation can lead to higher angle grain boundary and may induce the development of DRX grains.

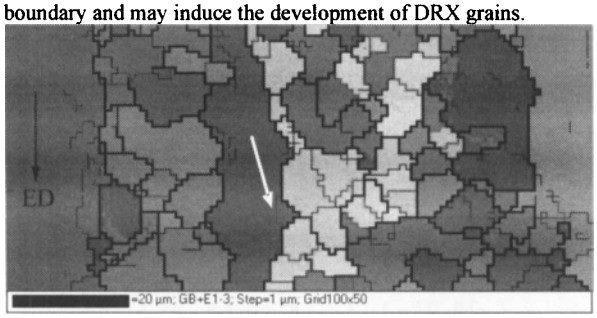

Figure 5. Orientation map of extruded rod (temperature=673K, velocity=0.8m/min). (Thick black line >15° misorientation, thin black line >10° misorientation, red thin line >5° misorientation, blue thin line>3° misorientation.)

Once the "necklace" structure forms along pre-existing grain boundary, dynamic recrystallization grains in AZ31 alloy cease to grow up and consume original grains. This has been observed by other researchers [21]. Upon further deformation, the fraction of recrystallized material will accommodate a number of strains. The continuous strain-induced process is responsible for the increase in misorientation near the grain boundary of DRX grains (indicated by white arrows in Figure 6). This process in recrystallization grains will make the small grains finer.

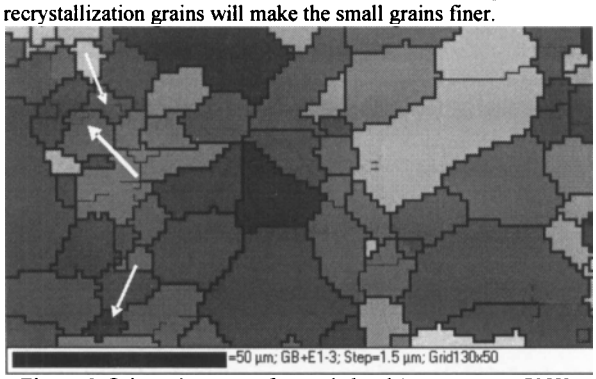

Figure 6. Orientation map of extruded rod (temperature=703K, velocity=1.4m/min). (Thick black line >15° misorientation, thin black line >10° misorientation, red thin line >5° misorientation, blue thin line>3° misorientation.)

Previous research showed that twin boundaries could act as sites for the nucleation of DRX grains [23,24]. Twinning related DRX is also observed in present study. As indicated by white arrow in Figure 7, twining with lens morphology has been subdivided into two grains. This can be attributed to the development of low angle boundaries that transformed to high angle boundaries caused by continuous straining.

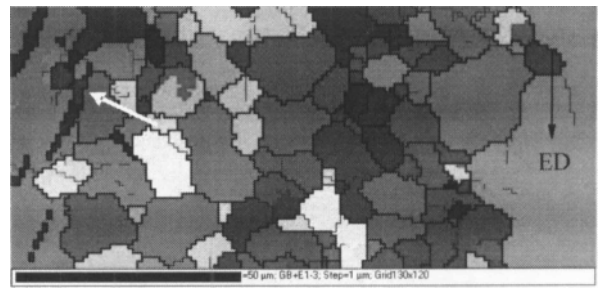

Figure 7. Orientation map of extruded rod (temperature=643K, velocity=0.8m/min). (Thick black line >15° misorientation, thin black line >10° misorientation, red thin line >5° misorientation, blue thin line>3° misorientation.)

Formation of Basal Texture

The texture evolution for the 9 different extrusion processes has also been studied by EBSD. Figure 8 presents the orientation distribution function (ODF) sections of casting billet, which do not show an obvious distribution pattern. As shown in Figure 9, there are strong (0002) fiber textures in the extruded AZ31 rods. This is in accord with the conclusion that fiber texture is usually formed for rods during uniaxial deformation of hexagonal structured metals [24]. However, texture component <0002> is not exactly parallel to the extrusion direction, the deviation is roughly 10°-20°.

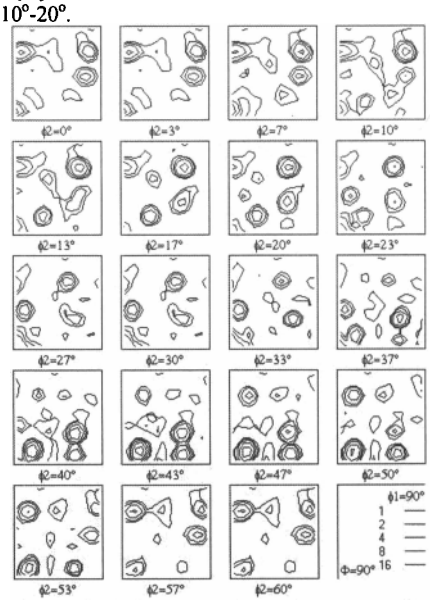

Figure 8. ODF measured from the as-cast billet.

Previous research [15] shows that $\{10\bar{1}2\}$ tension twining is favored at the early stage of deformation when the casting grain size is large, intensive twinning will reorient the initial grain orientation to a basal orientation. Once basal texture is formed, grains act as if they initially have a basal orientation during subsequent deformation.

Figure 3 shows that necklace DRX can gradually take place at the grain boundary. The DRX grains produced by buldging have orientations similar to those of the parent grains and serve to strengthen the basal texture, while nucleation brought by the

development of high angle grain boundary does not have such orientation correlation which tends to lead to random texture [25]. Furthermore, twinning and non-basal slip are in a competitive relation [26,27]. With the proceeding of deformation, twinning is suppressed and non-basal slip is activated because of the grain refinement caused by DRX. Non-basal slip also tends to reorient the basal texture towards the radial direction.

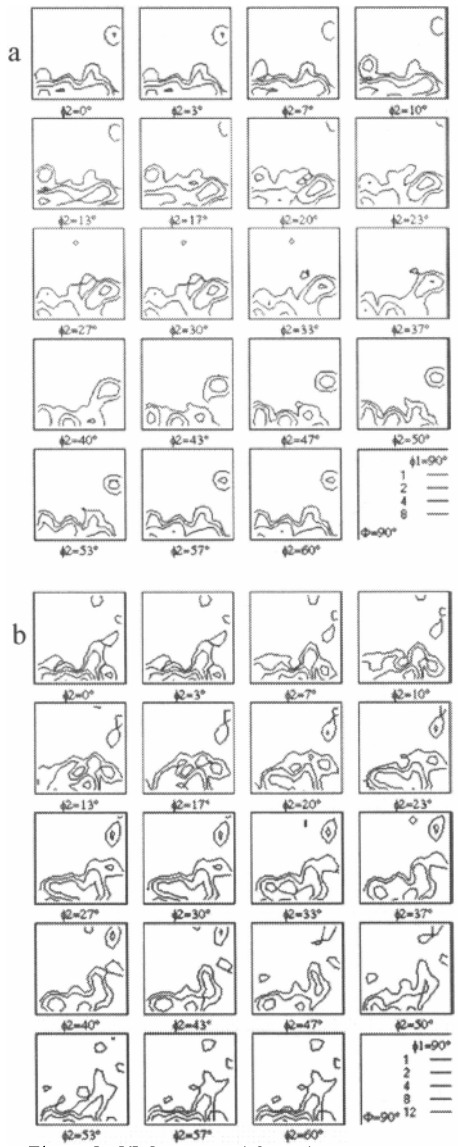

Figure 9. ODF measured from the as-cast billet. (a) Temperature=673K, velocity=0.8m/min. (b) Temperature =703K, velocity=2.2m/min.

Yield Strength Improvement

Grain refinement is proved to be effective in improving yield strength. As presented in Figure 10, average grain sizes of extruded rods decline dramatically compared with grain size of casting billet (about 200μm). Each value comes from the average of about 500 grains. The yield strength of casting billet is 83 Mpa.

As shown in Figure 11, yield strength was greatly improved (up to 200 to 210 MPa) by hot extrusion process. However, under the same extrusion temperature, yield strength of extruded rods decreases with increasing extrusion velocity, while average grain sizes of extruded rods are almost stable with increasing extrusion velocity. Hence, yield strength can not be solely described by average grain size.

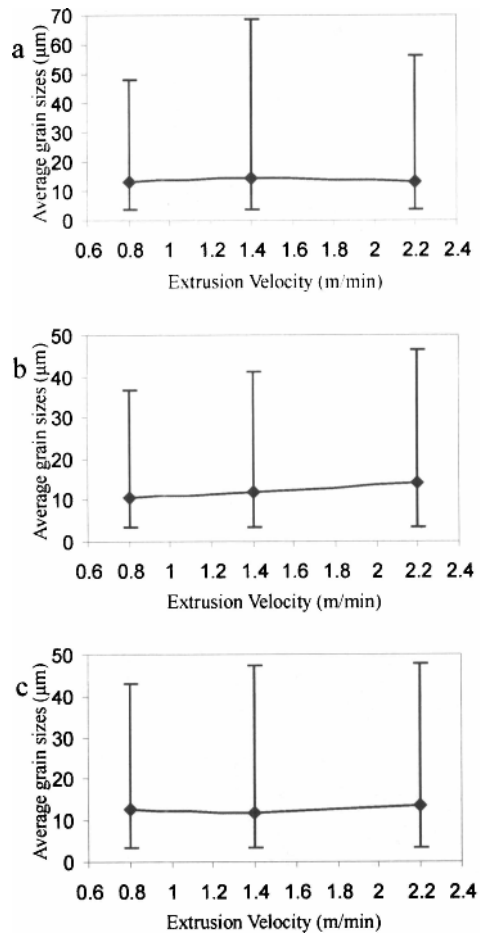

Figure 10. Average grain sizes of extruded rods (Measured by EBSD, transverse direction). (a) Temperature=643K. (b) Temperature=673K. (c) Temperature=703K.

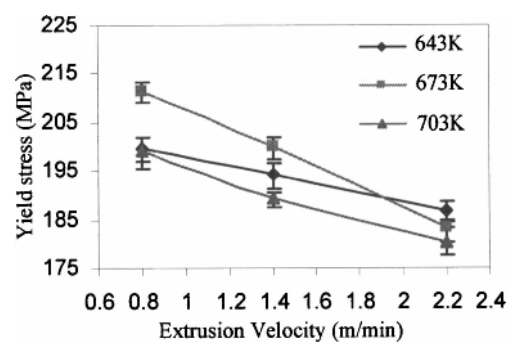

Figure 11. Yield strengths of extruded rods

In the current study, the influence of grain size and its orientation of each grain on yield strength is considered by applying Hall-Petch equation to each individual grain with the input of EBSD results. The procedure is summarized as follows.

The friction stress σ_0 in Hall-Petch equation is thought to be related to the deformation system with lowest yield strength [28] which depends on two factors: the critical resolved shear stress (CRSS) of the deformation system and grain orientation. For AZ31 alloy, the potential operative deformation systems are basal <a>, prismatic <a>, pyramidal <c+a> slip systems and tensile twinning systems. The yield strength σ_0 of deformation system α along the load direction is represented as σ_0^α:

$$\sigma_0^\alpha = \frac{\tau^\alpha}{P^\alpha} \tag{2}$$

where τ^α represents the CRSS of deformation system α, and P^α is Schmid factor, which is defined as

$$P^\alpha = \cos\theta \cdot \cos\varphi \tag{3}$$

where θ is the angle between the slip/twinning direction and the stress axis, and φ is the angle between the slip/twinning plane normal and the stress axis. The yield strength of individual grain σ_c is defined as

$$\sigma_c = \min(\sigma_0^\alpha) + k d_c^{-1/2} \tag{4}$$

where $\min(\sigma_0^\alpha)$ represents lowest yield strength among all deformation systems. For grains with different orientations and grain sizes, the yield strength of individual grain σ_c can be different. By employing Taylor assumption, the yield strength of polycrystal σ_M is calculated as the average of σ_c:

$$\sigma_M = < \sigma_c > \tag{5}$$

In this formulation, several parameters are required to calculated σ_c, including the critical resolved shear stress τ^α, Schmid factor P^α, slope k and individual grain size d_c. The individual grain size d_c and Schmid factor P^α can be obtained with the input of EBSD results (grain size and Eulerian angles). The remaining unknown parameters are CRSS τ^α and slope k, which can be obtained by parameters fitting. However, the CRSSs differ significantly for different deformation systems in AZ31 alloy, suggesting four different CRSS values are necessary. Combining with slope k, five parameters can lead to a difficulty in determining values by parameters fitting. To simplify the fitting procedure, CRSS ratio is set to basal <a>:prismatic <a>:pyramidal <c+a>: tensile twinning = 1:8.8:11.1:5.2 according to the recent research on AZ31 alloy [29,30]. Here, the CRSS values are normalized by the CRSS of basal <a> slip.

Based on the above fitting procedure, slop k has a value of 12 Mpa·mm$^{-1/2}$, and CRSS of basal <a> slip is 7.5 Mpa. The CRSSs for other deformation systems can be calculated by its ratio to basal slip. Figure 12 plots the yield strength obtained from this fitting method. Under the same extrusion temperature, the calculated yield strength decreases with the increase of extrusion velocity. This is similar to the experiment result. However, the value predicted by the fitting method is not exactly the same as experiment result (The largest deviation is 8.8Mpa, where the extrusion condition is 673k, 0.8m/min). This is possibly caused by the insufficient amount of individual grain data since each fitted value comes from 500 grains. A better result can be obtained if a larger number of grain size and orientation is available.

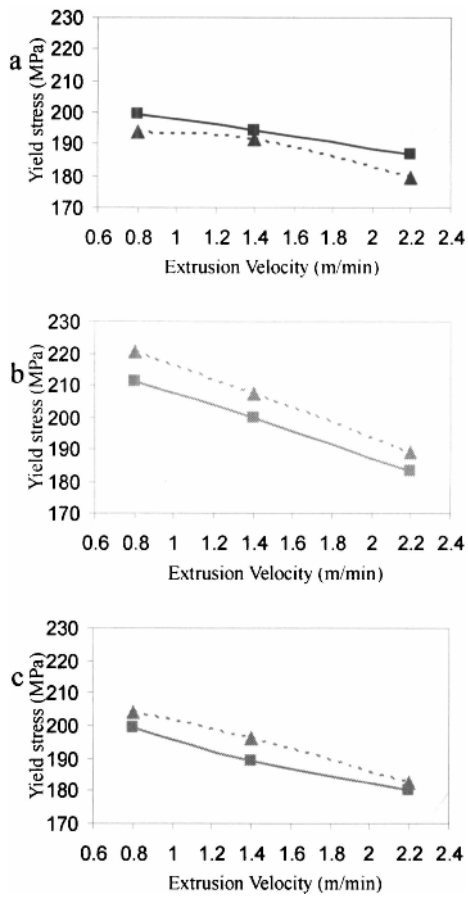

Figure 12. Yield strengths of extruded rods (Experiment Value: thick line and rectangular symbol, fitted value: dashed line and triangle symbol). (a) Temperature=643K. (b) Temperature=673K. (c) Temperature=703K.

Summary

In this paper, the effects of hot extrusion process on microstructure development, texture evolution and tensile properties of AZ31 alloy were studied. The following conclusions were drawn:

1. The extruded microstructures are very inhomogeneous with average grain size decreasing dramatically which can be attributed to DRX process. DRX grains can be generated in pre-existing grain boundaries, DRX grain boundaries and twinning boundaries.
2. The extruded AZ31 rods have basal planes almost parallel to the extrusion direction within a certain degree. The texture evolution during extrusion process is influenced by twinning, slip and DRX collectively.
3. Yield strength is greatly improved by hot extrusion process. However, under the same extrusion temperature, yield strength of extruded rods decreases with increasing extrusion velocity, while average grain sizes of extruded rods are almost stable with increasing extrusion velocity. Hence, yield strength can not be solely described by average grain size. To get a better prediction of yield strength, EBSD data (individual grain size and

orientation) for individual grains with Taylor assumption (with a large data set) is helpful.

Acknowledgement

The authors are thankful to the assistance of Dr.J.Boileau on Optical Microscopy work. The authors are thankful to the work of Dr. M.Li on EBSD.

The authors from Shanghai Jiaotong University acknowledge the support from the National Natural Science Foundation of China (No. 51175335), Ministry of Education of China (No.311017), Shanghai Science & Technology Projects (No.10QH1401400, 10520705000, 10JC1407300), and University Research Program of Ford Motor Company. The authors also appreciate the supported of the Research Fund of State Key Laboratory of China (No MSV-MS-2010-05).

References

1.H. Somekawa and T. Mukai, "Effect of texture on fracture toughness in extruded AZ31 magnesium alloy," *Scripta Materialia*, 53(2005), 541-545.

2.W.J. Kim et al., "Texture development and its effect on mechanical properties of an AZ61 Mg alloy fabricated by equal channel angular pressing," *Acta Materialia*, 51(2003), 3293-3307.

3.Y. Uematsu et al., "Effect of extrusion conditions on grain refinement and fatigue behaviour in magnesium alloys," *Materials Science and Engineering A*, 434(2006), 131-140.

4.V.J. del, F. Carreno, and O.A. Ruano, "Influence of texture and grain size on work hardening and ductility in magnesium-based alloys processed by ECAP and rolling," *Acta Materialia*, 54(2006), 4247-4259.

5.G.B. Hamu, D. Eliezer, and L. Wagner, "The relation between severe plastic deformation microstructure and corrosion behavior of AZ31 magnesium alloy," *Journal of Alloys and Compounds*, 468(2009), 222-229.

6.G.G. Yapici and I. Karaman, "Common trends in texture evolution of ultra-fine-grained hcp materials during equal channel angular extrusion," *Materials Science and Engineering A*, 503(2009), 78-81.

7.L. Jin et al., "Microstructure evolution of AZ31 Mg alloy during equal channel angular extrusion," *Materials Science and Engineering A*, 423(2006), 247-252.

8.J. Swiostek et al., "Hydrostatic extrusion of commercial magnesium alloys at 100 C and its influence on grain refinement and mechanical properties," *Materials Science and Engineering A*, 424(2006), 223-229.

9.J. Bohlen et al., "Microstructure and texture development during hydrostatic extrusion of magnesium alloy AZ31," *Scripta Materialia*, 53(2005), 259-264.

10.Y.J. Chen et al., "Microstructure evolution in magnesium alloy AZ31 during cyclic extrusion compression," *Journal of Alloys and Compounds*, 462(2008), 192-200.

11.K. Mueller and S. Mueller, "Severe plastic deformation of the magnesium alloy AZ31," *Journal of Materials Processing Technology*, 187-188(2007), 775-779.

12.S.S. Park, B.S. You, and D.J. Yoon, "Effect of the extrusion conditions on the texture and mechanical properties of indirect-extruded Mg-3Al-1Zn alloy," *Journal of Materials Processing Technology*, 209(2009), 5940-5943.

13.M. Shahzad and L. Wagner, "Influence of extrusion parameters on microstructure and texture developments, and their effects on mechanical properties of the magnesium alloy AZ80," *Materials Science and Engineering A*, 506(2009), 141-147.

14.V.J. del, F. Carreno, and O.A. Ruano, "Influence of texture and grain size on work hardening and ductility in magnesium-based alloys processed by ECAP and rolling," *Acta Materialia*, 54(2006), 4247-4259.

15.Y.N. Wang and J.C. Huang, "The role of twinning and untwinning in yielding behavior in hot-extruded Mg-Al-Zn alloy," *Acta Materialia*, 55(2007), 897-905.

16.S. Graff, W. Brocks, and D. Steglich, "Yielding of magnesium: From single crystal to polycrystalline aggregates," *International Journal of Plasticity*, 23(2007), 1957-1978.

17.L.L. Chang et al., "Grain size and texture effect on compression behavior of hot-extruded Mg-3Al-1Zn alloys at room temperature," *Materials Characterization*, 60(2009), 991-994.

18.N.J. Petch, "The cleavage strength of crystals," *Journal of the Iron and Steel Institute*, 174(1953), 25-28.

19.E.O. Hall, "The Deformation and Ageing of Mild Steel: III Discussion of Results," *Proceedings of the Physical Society. Section B*, 64(1951), 747-753.

20.B.S. Fromm et al., "Grain size and orientation distributions: Application to yielding of -titanium," *Acta Materialia*, 57(2009), 2339-2348.

21.S.M. Fatemi-Varzaneh, A. Zarei-Hanzaki, and H. Beladi, "Dynamic recrystallization in AZ31 magnesium alloy," *Materials Science and Engineering A*, 456(2007), 52-57.

22.A.G. Beer and M.R. Barnett, "Microstructural development during hot working of Mg-3Al-1Zn," *Metallurgical and Materials Transactions A: Physical Metallurgy and Materials Science*, 38(2007), 1856-1867.

23.A.G. Beer and M.R. Barnett, "The influence of twinning on the hot working flow stress and microstructural evolution of magnesium alloy AZ31," *Materials Science Forum*, 488-489(2005), 611-614.

24.I.L. Dillamore and W.T. Roberts, "Preferred orientation in wrought and annealed metals," *Metallurgical Reviews*, 10(1965), 271-380.

25.D. Ponge and G. Gottstein, "Necklace formation during dynamic recrystallization: Mechanisms and impact on flow behavior," *Acta Materialia*, 46(1997), 69-80.

26.M.R. Barnett et al., "Influence of grain size on the compressive deformation of wrought Mg-3Al-1Zn," *Acta Materialia*, 52(2004), 5093-5103.

27.Y. Chino et al., "Mechanical anisotropy due to twinning in an extruded AZ31 Mg alloy," *Materials Science and Engineering A*, 485(2008), 311-317.

28.R.W. Armstrong, "Theory of the tensile ductile-brittle behavior of poly-crystalline h.c.p. materials, with application to beryllium," *Acta Metallurgica*, 16(1968), 347-355.

29.B. Raeisinia, S.R. Agnew, and A. Akhtar, "Incorporation of solid solution alloying effects into polycrystal modeling of Mg alloys," *Metallurgical and Materials Transactions A: Physical Metallurgy and Materials Science*, 42(2011), 1418-1430.

30.H. Wang et al., "Evaluation of self-consistent polycrystal plasticity models for magnesium alloy AZ31B sheet," *International Journal of Solids and Structures*, 47(2010), 2905-2917.